APPENDIX: ERROR ANALYSIS

To evaluate the amount of the error induced in the diffusivity values by the multiple differentiations and integrations that were performed numerically on the experimental data, the computational scheme was used to analyze some artificial data with a known constant diffusivity. The data were generated by solving the special case of Equation (6) in cylindrical coordinates in which v_z, D, and ρ were all constant. Equation (6) then can be reduced to

$$\frac{\partial}{\partial z}\rho_A = \frac{1}{\alpha}\left[\frac{1}{r}\frac{\partial}{\partial r}r\frac{\partial \rho_A}{\partial r} + \frac{\partial^2}{\partial z^2}\rho_A\right] \tag{A1}$$

where $\alpha = v_{z/D}$

The appropriate boundary conditions are

$$\left.\frac{\partial \rho_A}{\partial r}\right|_{r=1} = 0 = \left.\frac{\partial}{\partial r}\rho_A\right|_{r=1} \tag{A2}$$

$$\lim_{z\to\infty}[\rho_A] = \rho_{A\text{mean}}$$

The set of Equations (A1) and (A2) has the solution as given by Bernard and Wilhelm (*20*),

$$\rho_A(r, z) = \rho_{A\text{mean}} + \sum_{n=0}^{\infty}\left[\frac{\alpha_e[\alpha - (\alpha^2 + 4\beta_n^2)^{1/2}]^{z/2}}{J_o^2(\beta_n R_o)\,(\alpha^2 + 4\beta_n^2)^{1/2}}\right] J_o(\beta_n r) \tag{A3}$$

where the β_n are the roots of

$$J_1(\beta_n R_o) = 0 \tag{A4}$$

Equation (A3) was used to generate concentration profiles for various values of $\alpha = v_{z/D}$. This data was then analyzed by the numerical scheme that was devised for the evaluation of Equation (10) and the resulting values of $D_r(r^*)$ compared with the theoretical value that had been used to generate the data. The entire process was repeated twice with random error of 0 to 10% and 0 to 20% being added to the concentration values. This was done to simulate the presence of experimental error in the actual data. The results of these computations are shown in Figure 17 for one particular value of α, and the deviation at each radial position is indicated. These results demonstrate that the numerical procedure has the greatest deviation at the center of the bed and near the edges. This is expected since the denominator of Equation (10) approaches zero in these regions.

As can be seen from Figure 17, the addition of random error does not cause rapid generation of instabilities in the computed results, and up to 20% error in the concentration data can be handled by the program.

The Flow Characteristics of Swirl (Centrifugal) Spray Pressure Nozzles with Low Viscosity Liquids

NORMAN DOMBROWSKI and DAVID HASSON

Imperial College, London, England

A study has been made of the mechanics of flow of low viscosity liquids through swirl spray nozzles. Discharge coefficients and spray angles have been measured for a series of nozzles designed to systematically determine dimensional effects not predicted by frictionless theory, in particular the effect of the ratios of swirl chamber diameter to orifice diameter and of orifice length to orifice diameter. It was found that a unique relationship exists between discharge coefficient and spray angle dependent only upon the value of the orifice length/diameter ratio. This result has been explained on the basis of an ideal flow theory extended to take into account the frictional decay of the vortex motion. A general expression has been derived which permits correlation of the flow characteristics of nozzles covering a wide range of designs.

Swirl (or centrifugal) spray pressure nozzles are probably the commonest type of atomizer to be found in industry and numerous fundamental studies have been carried out in order to relate the spray angle and discharge coefficient to the nozzle dimensions. However, except under very limited conditions none of the present theories is sufficiently reliable and for most applications design methods follow empirical lines.

Published data is inadequate to allow accurate assessments to be made of the effect of nozzle dimensions on the flow characteristics, information on the spray angle being particularly meager. Further data have therefore been collected using a series of about 80 accurately manufactured nozzles. A theory is presented which extends the range of existing design methods for low viscosity liquids and allows the correlation of the flow characteristics of a range of nozzle designs.

Norman Dombrowski is at The University, Leeds, England. David Hasson is at The Technion, Haifa, Israel.

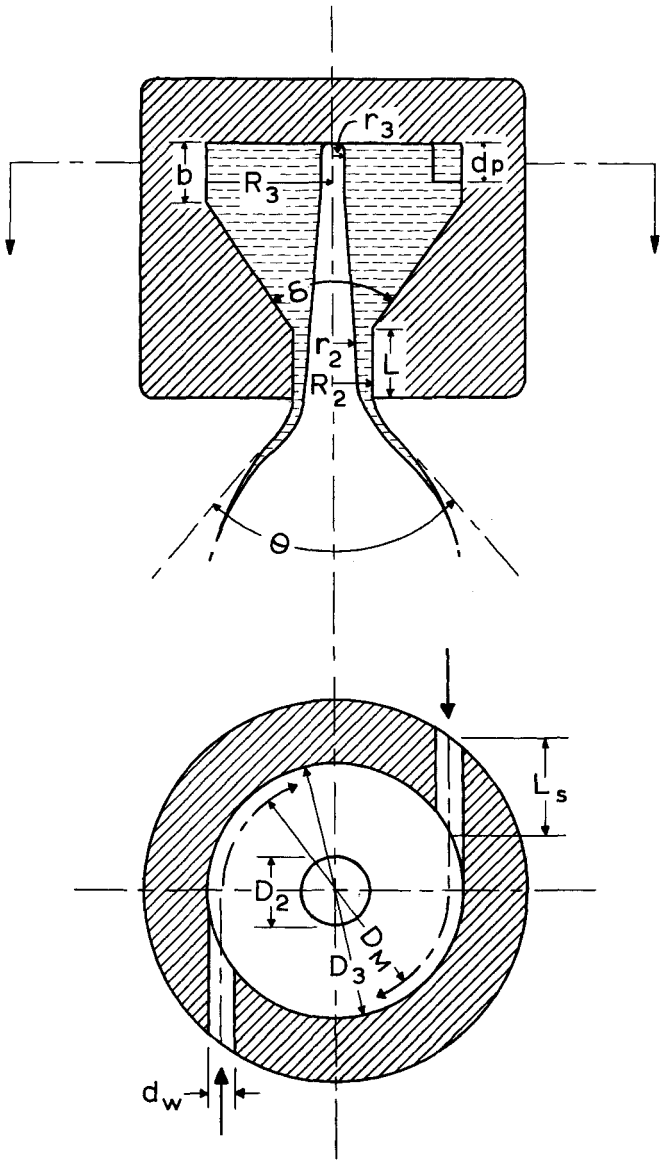

Fig. 1. Schematic diagram of a swirl spray nozzle.

THEORIES OF FLOW THROUGH SWIRL SPRAY NOZZLES

In a swirl spray nozzle, liquid is introduced through tangential or helical passages into a swirl chamber from which it emerges through a final orifice with a tangential velocity component (Figure 1). As a consequence of the vortex flow, a hollow air core is formed concentric with the nozzle axis. The outflowing thin conical sheet attenuates rapidly, becomes unstable and disintegrates into drops.

The motion within the swirl chamber is complex. Taylor (*1*) has shown that although the motion in the main stream can be considered irrotational, the viscous effect of the retarded boundary layer is far from negligible. The liquid in contact with the atomiser walls cannot rotate fast enough to hold it in a circular path against the radial pressure gradient balancing the centrifugal motion and consequently, a current directed towards the orifice is set up through the surface layer.

The analysis has been extended and refined by other workers (*2* to *4*) and it has been shown (*3*) that outward flow may also occur through a boundary layer around the air core. Experimental studies (*5* to *7*) have also revealed that under certain conditions reverse axial flow can take place in the upper part of the nozzle. At this stage, theories of flow of real fluids are not readily applicable for design purposes. However, for low viscosity liquids, useful information as to the controlling parameters can be obtained on the basis of ideal flow.

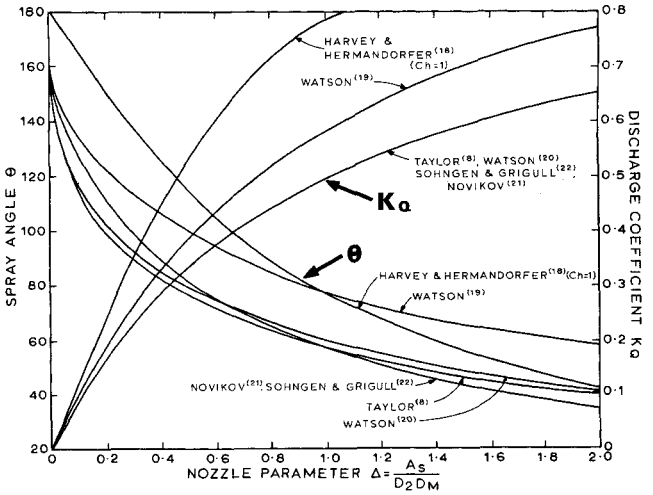

Fig. 2. Variation of θ and K_Q with Δ according to various theories.

Theories assuming frictionless flow are based on the equations of continuity, conservation of angular momentum, and of conservation of energy.

The most satisfactory solution of these equations has been obtained by Taylor (*8*) who found that $K_Q = K_Q\{y\}$ and $\theta = \theta\{x, y, z.\}$ The relationship of Taylor's functions with the dimensions of the nozzle is obtained by equating the flow at entry with the flow at exit, that is

$$Q = A_s V_3 = \pi R_2^2 U_P K_Q \qquad (1)$$

It can be easily shown that the effective radius correspond-

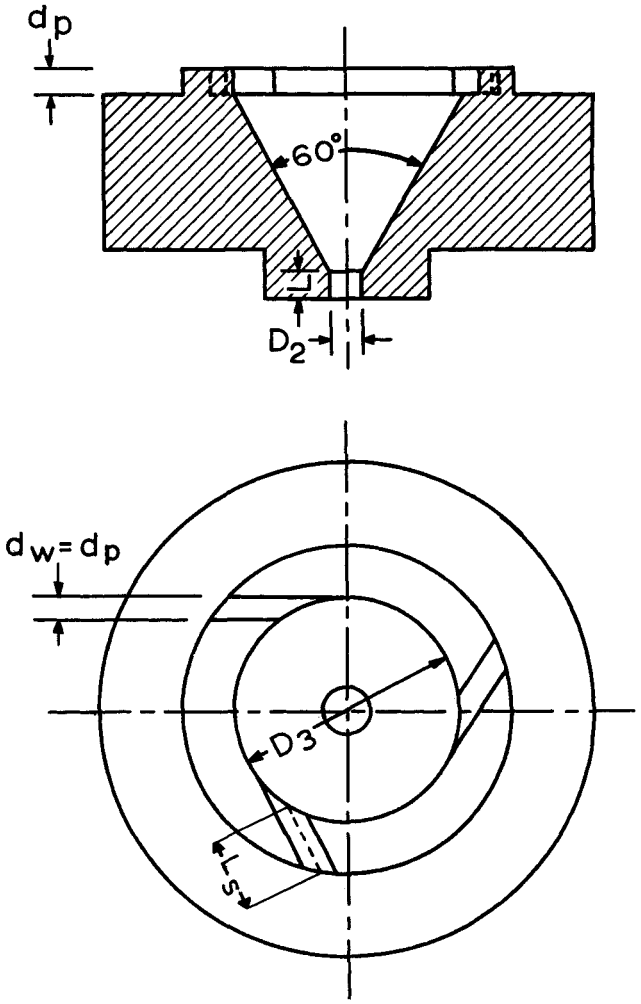

Fig. 3. Design features of experimental nozzle. (D_3/d_w = 9, L_s/d_w = 3). (flow number range, Imperial gal./hr./$\sqrt{}$lb./sq. in., = 1 — 10).

ing to the velocity V_3 in the swirl grooves is $R_M = R_3 - d_w/2$

Hence from Equation (1)

$$V_3 = \text{constant} \times R_M^{-1} \quad (2)$$

Combining Equations (1) and (2) gives

$$\frac{\pi K_Q}{4y} = \frac{A_s}{D_2 D_M} = \Delta \quad (3)$$

It is thus seen that for the flow of an ideal fluid, both the discharge coefficient K_Q and the spray cone angle θ are unique functions of the nozzle parameter Δ and independent of the inlet pressure.*

Figure 2 shows the functional relationships between Δ, θ, and K_Q of Taylor and a number of other workers. The differences originate in the simplifying assumptions made, some of which are invalid (9).

DESIGN OF EXPERIMENTAL SWIRL SPRAY NOZZLES

Published data indicate that nozzle dimensions, other than those already expressed by the ideal theory parameter Δ, affect the flow characteristics, but apparent inconsistencies make it impossible to establish any useful relationships; moreover, information on the initial spray angle as defined by theory is sparse, since most investigators have only measured the effective angle of the spray some distance from the nozzle. Further data have therefore been collected using a series of accurately manufactured nozzles.

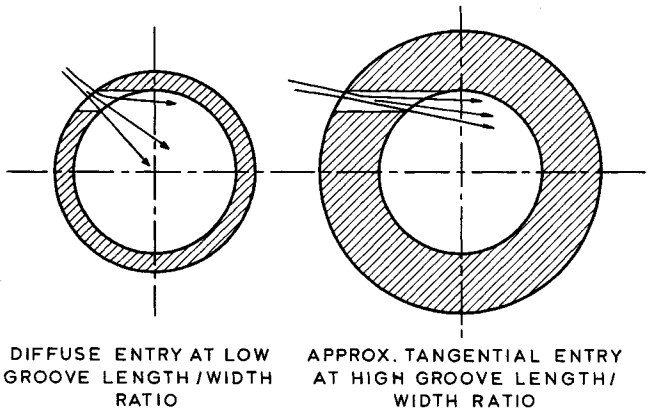

Fig. 5. Influence of groove length/width ratio on flow in swirl chamber.

The nozzle type, selected for investigation, is illustrated in Figure 3 and its assembly is shown in Figure 4.

Although circular grooves are easier to drill to within specified limits of accuracy, this advantage is outweighed by the practical difficulties in obtaining holes which are truly tangential to the chamber. Noncircular grooves were therefore selected, a square cross section being arbitrarily chosen. The value of the groove length/width ratio (L_s/d_w) must be sufficiently large to ensure that the liquid enters the chamber tangentially and not by diffuse flow, as illustrated in Figure 5. It must not, however, be too large, since the gain in circulation may be offset by frictional loss. A pilot experiment was therefore carried out to determine the value of the optimum ratio at which frictional losses are a minimum (that is maximum angle, minimum discharge coefficient). The results indicated an optimum value of L_s/d_w of 3 and this value was chosen for the design of the subseqent nozzles. The swirl chamber diameter/groove width ratio can similarly be expected to affect the circulation generated in the liquid entering the swirl chamber. From a study of commonly used dimensions it was decided to maintain D_3/d_w constant at the value of 9.

A series of 81 nozzles was manufactured to allow determination of the effects of the variables Δ, D_2, D_M/D_2, and L/D_2 at the levels shown in Table 1. Two sets of the 0.081 in. orifice diameter nozzles were manufactured to assess deviations due to unavoidable manufacturing imperfections. Five nozzles, additional to the series, were also made in order to examine the effect of large orifice diameters and to extend the range into smaller values of Δ.

The flow characteristics of a swirl spray nozzle are greatly influenced by the precision of its manufacture. The dimensions were measured to $\pm$ 0.001 in. and nozzles were discarded with orifice eccentricity (Figure 6*b*) greater than 0.03 in. and mean tangent errors (Figure 6*a*) greater than 0.004 in. The inner surfaces were carefully polished and the grooves and orifices carefully examined for burrs and machining marks. The dimensions of the nozzles are given elsewhere (9).

Table 1*a*. Scheme of Systematic Series of Swirl Spray Nozzles

D_2 in. $\pm$ 0.001		0.081			0.120		
	N	3	6	9	3	6	9
$\frac{L}{D_2} \pm 0.025$	$\frac{D_M}{D_2} \pm 2\frac{1}{2}\%$	Δ ($\pm$ 5%)					
0.125 0.51 0.91	2.67	0.117	0.232	0.354	0.117	0.232	0.354
0.125 0.51 0.91	5.33	0.117	0.484	0.722	0.117	0.484	0.722
0.125 0.51 0.91	8	0.354	0.722	0.91	0.354	0.722	0.91

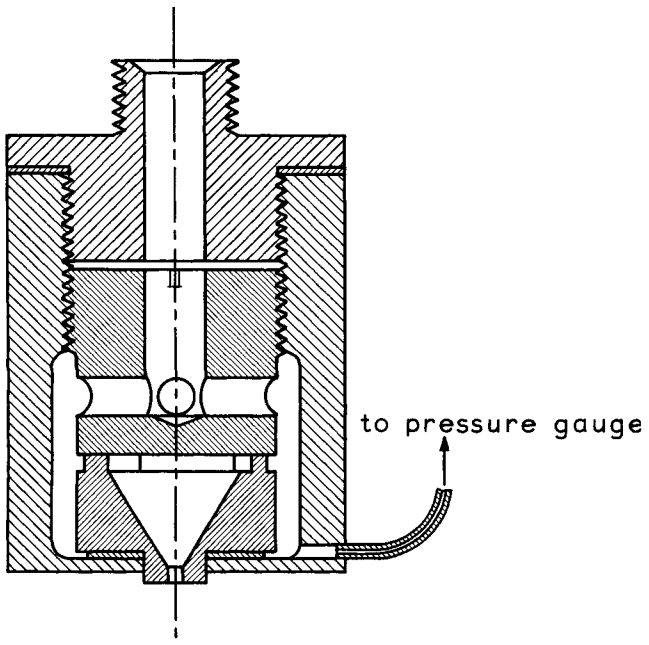

Fig. 4. Nozzle assembled in holder.

* Most authors have correlated their results against $\Delta' = (A_s/D_2D_3)$ which implies that in Equation (2) the radius of the inlet vortex is R_3 rather than R_M. This approximation is valid only for $d_w << D_3$.

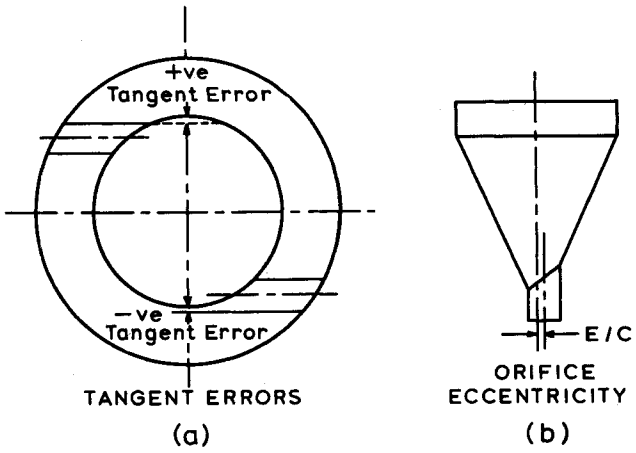

spray nozzles.

Fig. 6. Asymmetry faults in swirl spray nozzles.

Layout of Apparatus and Method of Measurement of Flow Characteristics

The tests consisted of measuring the flow rate and spray angle for each nozzle at a pressure of 50, 100, and 150 lb./sq.in. gauge, using water at room temperature.

The layout of the apparatus is shown in Figure 7. The liquid was ejected by applying compressed air, the pressure being accurately controlled by a reducing valve. The ejection pressure was measured, according to standard practice, at a point just outside the nozzle holder. In order to confirm that this pressure represented the total head of the liquid just upstream of the swirl grooves, it was compared in a few cases with the stagnant liquid pressure obtained at a point inside the nozzle holder, shown in Figure 4. The difference was found to be negligibly small, being less than 1 lb./sq.in. at the highest flow rates.

Nozzle output was measured by weighing a vessel containing the liquid collected for a known time. The spray was caught with minimum loss using a covered funnel having a circular inlet, into which the liquid was directed. The funnel was pivoted and could be swivelled quickly to its spray collecting position. Repeat tests, including experiments in which the same nozzle was dismantled and reassembled, showed satisfactory agreement, the reproducibility being well within 1%.

The spray angles were obtained from photographic negatives, taken at an exposure time of 1/30 sec. The angle measured is the one defined by theory, namely the maximum angle formed by tangents to the curving sheet in the vicinity of the orifice (Figure 8). This may differ considerably from the profile of the spray curtain or the spatial distribution of the drops which are affected by the ambient conditions.

RESULTS

Radcliffe (*10*) has studied the effects of differential ejection pressure, orifice diameter, and liquid properties on the flow characteristics of swirl spray nozzles and correlated his results by dimensional analysis. His curves, redrawn to express K_Q as a function of Reynolds number (defined by $D_2U_p\rho_L/\eta$), predict small variations at high Reynolds numbers. This is confirmed in the present work

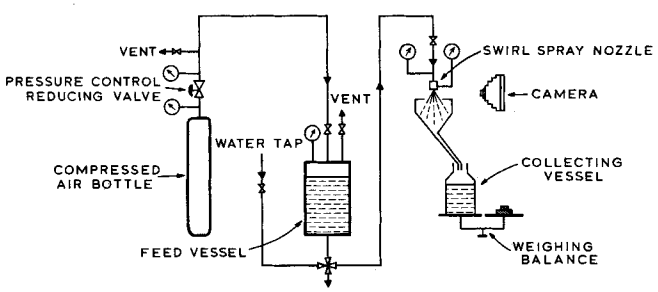

Fig. 7. Layout of apparatus.

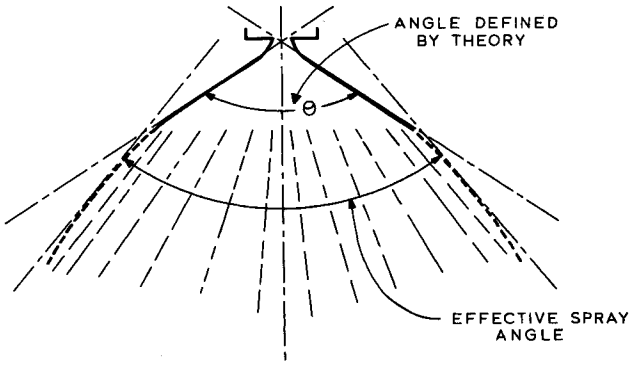

Fig. 8. Spray angle defined by theory.

where similar levels have been involved and subsequent discussion will therefore be restricted to pressures of 100 lb./sq.in. gauge with the small D_2 effects being neglected.

Values of K_Q and θ are plotted against Δ in Figures 9 and 10 respectively. Each experimental point represents an arithmetic mean of values obtained from three nozzles having the same nominal Δ, D_M/D_2, and L/D_2, two of the nozzles being nominal replicates. It is seen that the points are segregated according to the value of D_M/D_2 and L/D_2, the discharge coefficient increasing with increasing D_M/D_2 and diminishing L/D_2 while the spray angle diminishes with both increasing D_M/D_2 and L/D_2. Values of K_Q and θ are either above or below the Taylor ideal theory curve, depending on the magnitude of D_M/D_2 and L/D_2. This is not in accord with the generalization which is sometimes made, that the discharge coefficient is always higher while the angle is always lower than predicted by theory. In fact, the measured flow characteristics are much closer to the theoretical curve than might have been anticipated from the data of previous workers (see Figure 18).

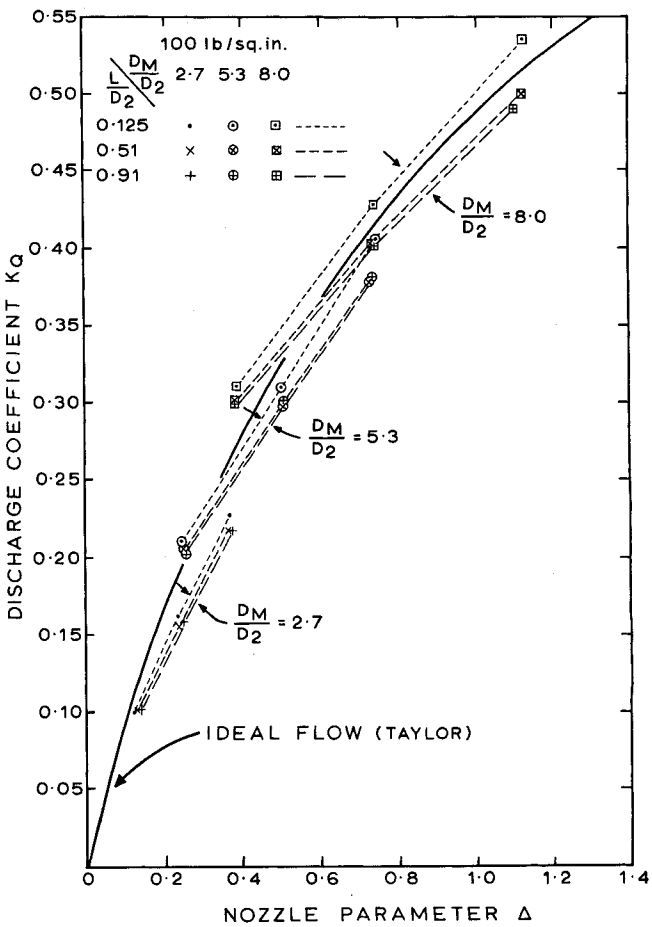

Fig. 9. Variation of K_Q with Δ.

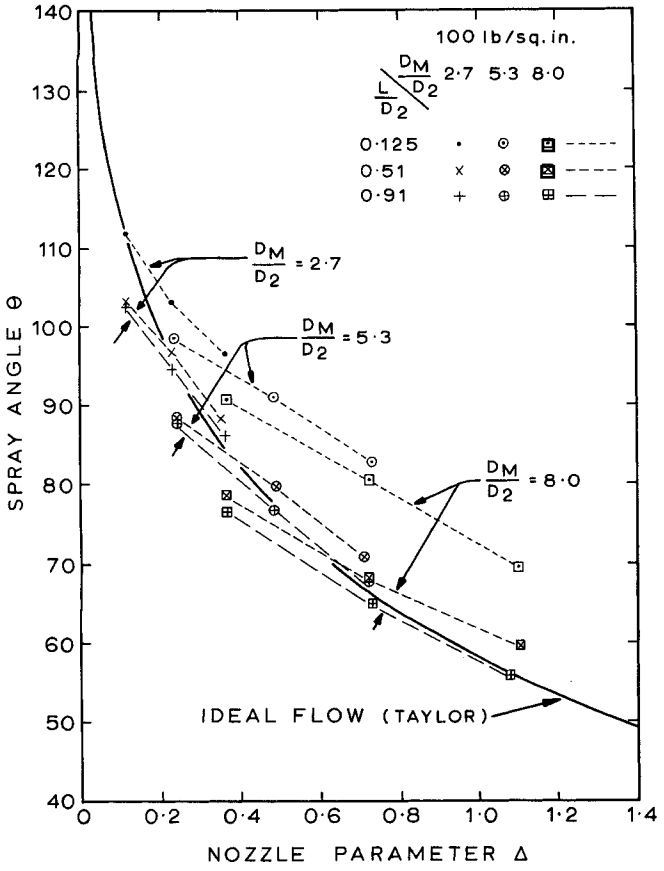

Fig. 10. Variation of θ with Δ.

A point of theoretical importance is discovered by plotting the discharge coefficient of each nozzle against its spray angle (Figure 11). It is found that for a given value of L/D_2, a unique relationship exists between K_Q and θ, independent of the variable D_M/D_2. This signifies that the variables Δ and D_M/D_2 are combined in one parameter. The additional nozzles of low Δ and high D_2 (Table 1*b*),

TABLE 1*b*. ADDITIONAL NOZZLES

D_2	Δ	$\frac{D_M}{D_2}$	$\frac{L}{D_2}$	N
0.120	0.036	2.83	0.126	3
0.120	0.062	2.77	0.133	3
0.120	0.078	2.73	0.126	3
0.189	0.118	2.67	0.128	3
0.265	0.124	2.66	0.135	3

belonging to the group $L/D_2 \approx 0.125$, have been included in Figure 11 and are seen to be consistent with the other points. These results can be explained as follows:

For an ideal liquid, conservation of angular momentum gives rise to a potential (or free) vortex so that

$$VR = \text{constant} \tag{4}$$

Numerous experimental investigations of the vortex motion of real fluids in cyclones [for example (*11*)] have established that the tangential velocity variation is best represented by the relationship,

$$VR^n = \text{constant} \tag{5}$$

where n is a fraction for which values between 0.5 to 0.84 have been quoted. This excludes the narrow region in the vicinity of the air core where n is almost -1.

It is therefore reasonable to conclude that an analysis of the flow inside a swirl spray nozzle, employing Equation (5) in place of Equation (4), should provide a more realistic indication of the controlling parameters. On this basis it can be shown (*9*) that

$$K_Q = K_Q \{\Delta(D_M/D_2)^{1-n}\} \tag{6}$$

and

$$\theta = \theta \{\Delta(D_M/D_2)^{1-n}\} \tag{7}$$

The analysis thus shows the nozzle variables Δ and D_M/D_2 to be combined in one parameter as suggested by the experimental results of Figure 11, although the extent of variation of each flow characteristic with D_M/D_2 depends on the magnitude of the frictional index n. The relationships between the flow variables for the case $n = \frac{1}{2}$ is compared with that for an ideal fluid ($n = 1$) in Figure 12.

In comparing theory with experiment it is assumed that the same value of n applies to all nozzles of a particular type of design. To find n, the experimental results of Figures 9 and 10 have been replotted against $\Delta(D_M/D_2)^{1-n}$, using various values of n. The best correlation was obtained with $n = 0.4$ to 0.6 and the value 0.5 was selected.

Figures 13 and 14 show the plots of K_Q and θ respectively against $\Delta(D_M/D_2)^{1/2}$ and it is seen that the points are now segregated only according to the value of L/D_2. Comparison with the theoretical curves for $n = \frac{1}{2}$ shows that the observed discharge coefficients are lower and the observed spray angles higher than predicted.

Velocity losses occurring in the orifice are indicated by the variations of the flow characteristics with L/D_2. It is found that both K_Q and θ are diminished as L/D_2 is increased (Figures 13 and 14). These variations cannot be ascribed to an effect of L/D_2 on the friction in the vortex as measured by n, since a change in the value of n would result in K_Q and θ respectively altering in opposite directions.

The reduction of K_Q with increasing L/D_2 implies a frictional loss in axial velocity and would be followed by an increase in the corresponding spray angle, had the tangential velocity remained constant. The observed decrease in spray angle signifies that in fact the tangential velocity is also diminished proportionately to a greater

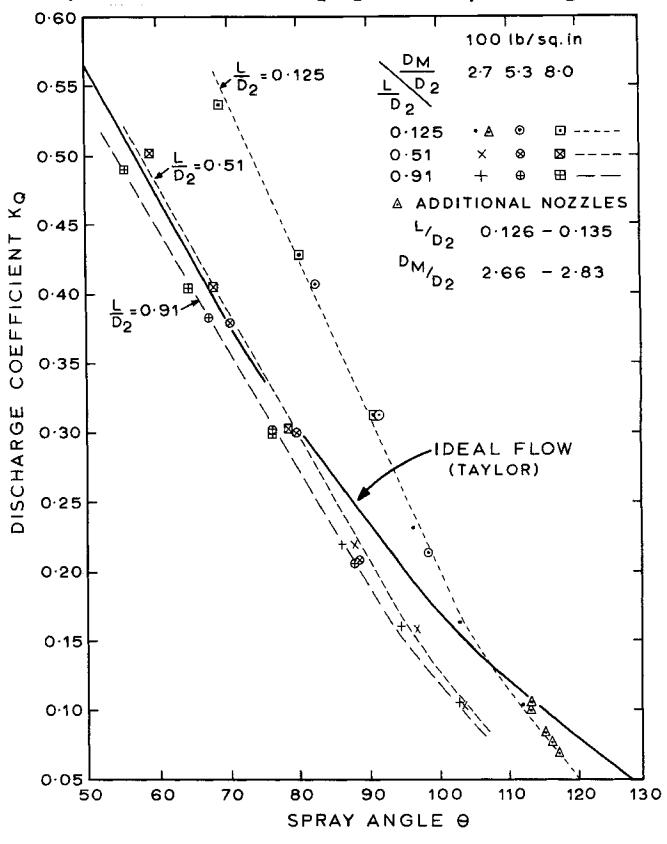

Relation between KQ and θ.

Fig. 11. Relation between K_Q and θ.

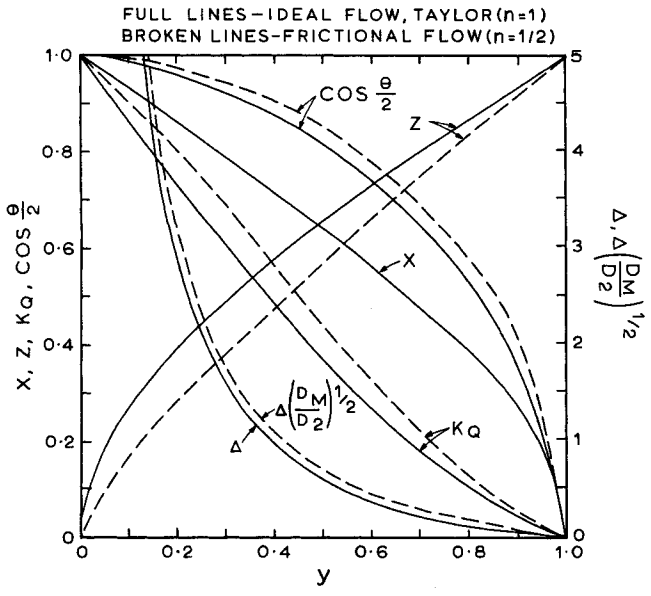

Fig. 12. Relations between flow variables.

extent than the axial component.

Frictional effects of this type should be manifested by pressure losses through the nozzle. An estimate of these losses can be obtained from the air-core data reported by Ellis (*12*). Values of K_V for water flow, have been calculated from the easily derived relationship:

$$K_V = \frac{K_Q}{K_A} = K_Q/[1 - (r_4/R_2)^2] \cos\frac{\theta}{2} \qquad (8)$$

and the results indicate that for $\Delta < 1$, $K_V < 0.8$. Stephens (*13*) has measured the total head of water at the orifice of a large nozzle of $\Delta = 0.05$ and found approximately two thirds of the inlet pressure to be lost through friction that is $K_V = 0.575$. Static pressure measurements obtained by Ellis with small nozzles, indicate that pressure losses occur at entry to the swirl chamber, in the chamber, and

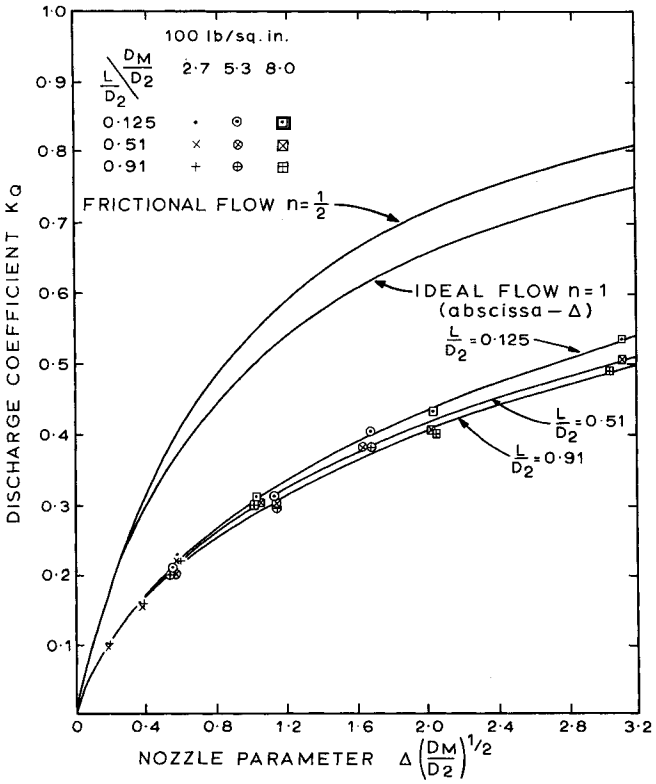

Fig. 13. Variation of K_Q with $\Delta\left(\frac{D_M}{D_2}\right)^{1/2}$.

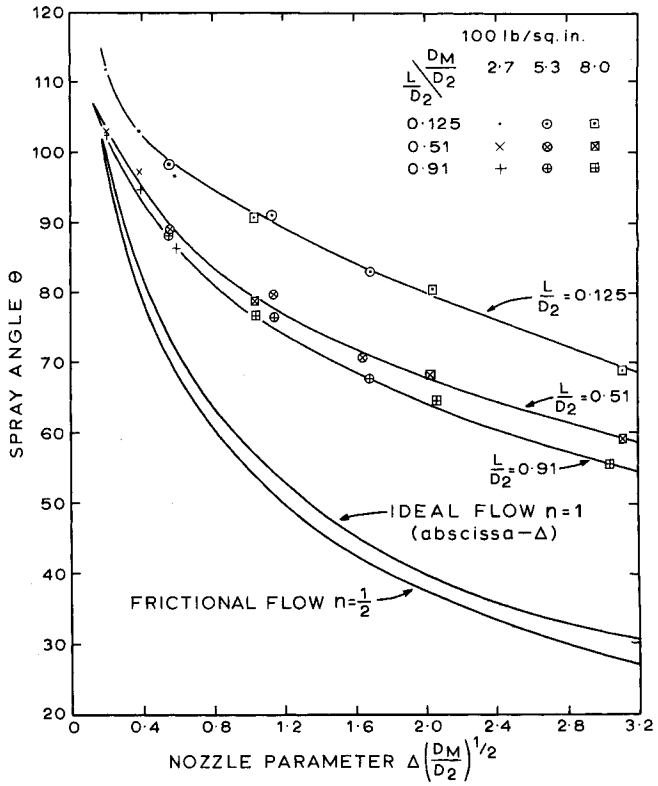

Fig. 14. Variation of θ with $\Delta\left(\frac{D_M}{D_2}\right)^{1/2}$.

in the orifice. His results show that at low values of Δ, entry losses contribute an appreciable proportion of the total loss but are negligible above a value of about 0.25.

Confirmation of these trends is indicated by some measurements made by the authors, by means of high speed photography, of the velocity of the coherent sheet. The results showed that for values of Δ of about 0.1, K_V is less than 0.6 while for values of Δ of about 1, K_V is approximately 0.9.

Application of Results to Design of Swirl Spray Nozzles

The success of the modified theory allows the use of

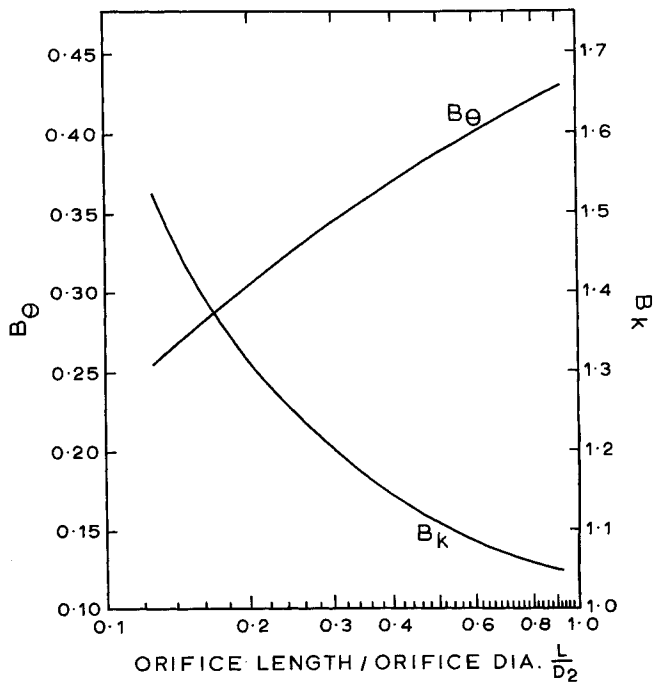

Fig. 15. Correction factors for $\frac{L}{D_2}$.

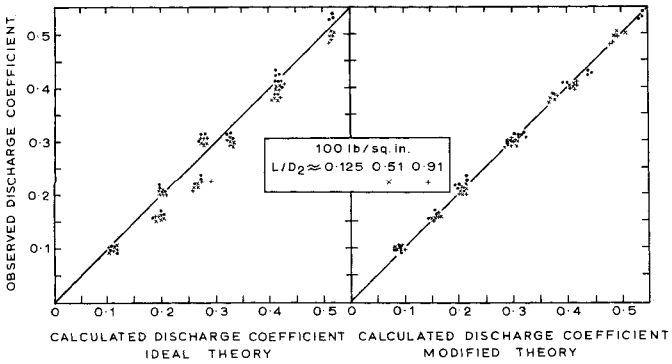

Fig. 16. Comparison of observed and calculated discharge coefficients.

simple empirical corrections for L/D_2.

The actual spray angle is directly obtained from the theoretical curve for $n = \frac{1}{2}$ (Figure 14), the nozzle parameter being modified to $B_\theta[\Delta(D_M/D_2)^{1/2}]^{2/3}$. This modified parameter is then used to obtain an apparent discharge coefficient, K_Q', from Figure 13, which is linearly related to the true discharge coefficient, K_Q, according to:

$$K_Q = B_K \cdot K_Q' - 0.05 \qquad (9)$$

Values of B_θ and B_K are plotted in Figure 15.

Figure 16*a* shows comparisons between the observed values of K_Q and values calculated according to the ideal theory for each of the 81 nozzles while Figure 16*b* shows comparisons with values calculated according to the modified theory. The corresponding plots for θ are given in Figure 17. It will be seen that calculations taking into account the effects of D_M/D_2 and L/D_2 give more satisfactory agreement, in particular for the spray angle.

Comparison between Results of Various Workers

To compare the results obtained by various workers, the discharge coefficients of nozzles having approximately similar values of D_M/D_2 and L/D_2 have been plotted against Δ in Figure 18. Details of the nozzle designs are given in Figure 19.

Figure 18 shows that the results of each author fall on a different curve. There is no identity even between Doble's (*14*) two curves relating to nozzles which are equal in all respects, except for the shape of the swirl grooves (circular in one case, rectangular in the other).

The sets of nozzles used in the various experimental investigations differed from each other in their overall geometry (Figure 19), and from comparisons of their flow characteristics, it is evident that there are large variations in frictional effects among nozzles of different designs. At present, it is not clear which particular nozzle dimensions are responsible. The ratios of several dimensions which may affect the flow characteristics, such as L_s/d_w and D_3/d_w, have been changed unsystematically, and the quality of surface finish, a further variable, may have differed. However, assuming that the main frictional difference between nozzles of various designs is in the vortex decay, as measured by n, it is found that the results of the various workers, covering a wider range of variables than is employed for Figure 18, can be made to coincide by selecting an appropriate value of n for each nozzle design. Figure 20 shows discharge coefficients plotted on this basis. Since variations in L/D_2 from 0 to 1 have only a small effect on the discharge coefficient, no attempt has been made to segregate the discharge coefficients according to L/D_2 levels.

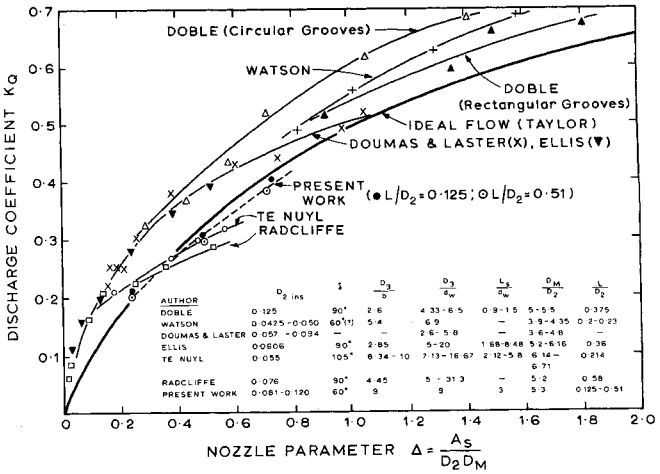

Fig. 18. Variations of K_Q with Δ for nozzles of various designs.

Radcliffe's (*10*) data for his nonstandard atomizers cannot, in general, be made to fall on a single curve by applying the new parameter. However, the nozzle design he used was fundamentally different, the inlet grooves being offset from the swirl chamber periphery (Figure 19*f*). This is in contrast to the other and more usual designs, (Figures 4, 19*a* to *e*) where care is taken to make the outer edge of the inlet grooves tangential to the periphery so as to minimize inlet flow disturbances. The data of Ellis (*12*) and Doble which show a wide scatter have also been excluded. The nozzles used by Ellis were reexamined by the present authors and a number were found to give nonuniform sprays and spray sheets of noncircular cross section; the scatter of Doble's results might be due to errors in manufacture, the quoted nozzle dimensions appearing to be specified and not measured values.

Here it may be noted that Doumas and Laster (*15*) obtained agreement between their observed discharge coefficients and those calculated according to the ideal flow theory by modifying empirically the nozzle parameter Δ' to $\Delta'(D_M/D_2)^{1/2}$. The latter resembles the present authors' analytically derived parameter $\Delta(D_M/D_2)^{1/2}$. However, there is no theoretical justification for replacing Δ by Δ', especially as in their nozzles the ratio Δ/Δ' reached the

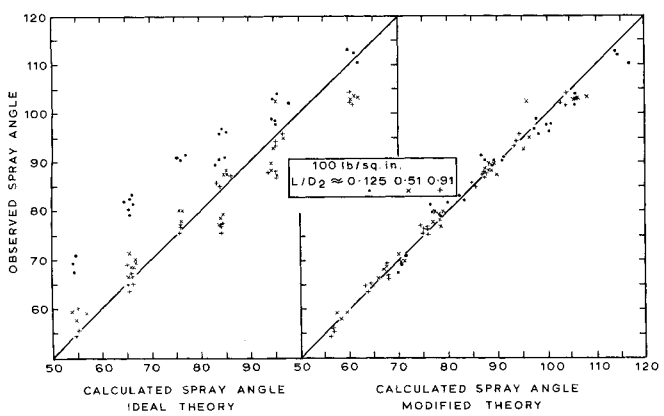

Fig. 17. Comparison of observed and calculated spray angles.

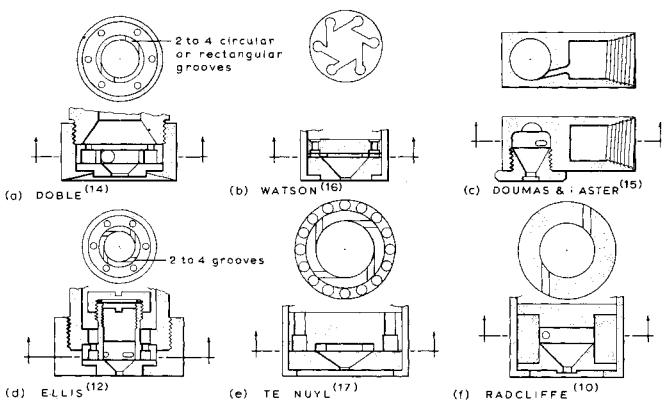

Fig. 19. Designs of nozzles used by various workers.

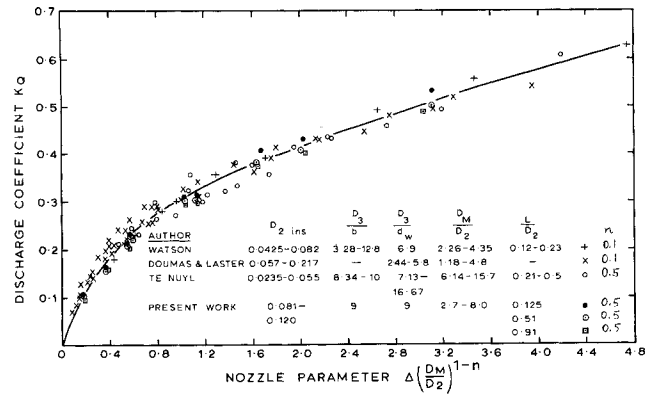

Fig. 20. Correlation of discharge coefficients.

high value of 1.6. The agreement with the ideal theory curve obtained by their correlation is by no means general; none of the other experimental curves coincides with the theoretical one, whether $\Delta(D_M/D_2)^{1/2}$ or $\Delta'(D_M/D_2)^{1/2}$ is used.

The significance of the new correlation becomes evident when spray angle data are examined (Figure 21).* Referring, for instance, to Watson's results (*16*) in Figures 20 and 21, it will be seen that the same value of n gives agreement for both discharge coefficient and spray angle.

Thus, for all practical purposes, the method of calculation suggested above may be applied to all nozzle designs, the only modification necessary being to adjust the value of n in the expression for the effective nozzle parameter.

ACKNOWLEDGMENT

Valuable discussions with Dr. P. Eisenklam and the late R. P. Fraser are gratefully acknowledged. The authors also wish to thank the Agricultural Research Council for financial support.

NOTATION

A_s = total area of swirl grooves
B_θ = correction factor for the effect of L/D_2 on the spray angle
B_K = correction factor for the effect of L/D_2 on the discharge coefficient
b = length of parallel portion of swirl chamber
C_h = air-core coefficient in Harvey and Hermandorfer's analysis
D_2 = orifice diameter
D_3 = swirl chamber diameter

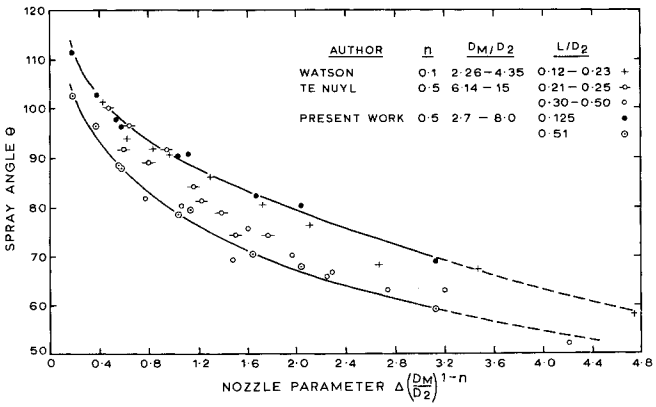

Fig. 21. Correlation of spray angles.

* Spray angles are more sensitive than discharge coefficients to small variations of L/D_2, and the curves are therefore segregated to within narrow limits of this variable.

The data of Doumas and Laster have not been utilized since the angles were measured by a volume-distribution method and therefore differ from that defined by theory.

D_M = mean diameter of inlet vortex in swirl chamber = $D_2 - d_w$
d_w = width of rectangular swirl groove
d_p = depth of rectangular swirl groove
K_A = area coefficient
K_V = velocity coefficient
K_Q = discharge coefficient
K_Q' = apparent discharge coefficient
L = orifice length
L_s = length of swirl grooves
N = number of swirl grooves
n = index of the frictional decay in vortex motion
Q = volume flow rate
R = radius at any point inside swirl spray nozzle
R_2 = orifice radius
R_3 = swirl chamber radius
R_M = mean radius of inlet vortex in swirl chamber
r_2 = air core radius in the orifice
r_4 = air core radius measured at the orifice exit plane
U_p = velocity corresponding to the total head
u_2 = axial velocity in the orifice
V = tangential velocity at any radius R inside nozzle
V_3 = tangential velocity at entry to the swirl chamber
x = dimensionless axial velocity ratio u_2/U_p
y = dimensionless circulation ratio, constant$/R_2U_p$ or constant$/R_2{}^nU_p$
z = dimensionless air-core ratio r_2/R_2

Greek Letters

Δ = dimensionless group of nozzle dimensions A_s/D_2D_M
Δ' = dimensionless group of nozzle dimensions A_s/D_2D_3
δ = cone angle of swirl chamber
η = absolute liquid viscosity
θ = spray cone angle
ρ_L = liquid density

LITERATURE CITED

1. Taylor, G. I., *Quart. J. Mech. Appl. Math.*, **3**, 129 (1950).
2. Binnie, A. M., and D. P. Harris, *ibid.*, **3**, 89 (1950).
3. Hodgkinson, T. G., *Porton Tech. Paper No. 191* (1950).
4. Cooke, J. C., *J. Aeronaut. Sci.*, **19**, 486 (1952).
5. Binnie, A. M., and J. D. Teare, *Proc. Roy. Soc.*, London, **A235**, 78 (1956).
6. ———, G. A. Hookings, and M. Y. M. Kamel, *J. Fluid Mech.*, **3**, 261 (1957).
7. Nissan, A. H., and V. P. Bresan, *AIChE J.*, **7**, 535 (1961).
8. Taylor, G. I., *Proc. 7th Intern. Congr. Appl. Mech.*, **2**, 280 (1948).
9. Hasson, D., Ph.D. thesis, London Univ., England (1956).
10. Radcliffe, A., *Proc. Inst. Mech. Eng.*, **169**, 93 (1955).
11. Stairmand, J. C., *Engineering*, **168**, 409 (1959).
12. Ellis, J. E., Ph.D. thesis, London Univ., England (1950).
13. Stephens, R. C., M.Sc. thesis, London Univ., England (1953).
14. Doble, S. M., *Proc. Inst. Mech. Eng.*, **157**, 103 (1947).
15. Doumas, M., and R. Laster, *Chem. Eng. Progr.*, **49**, 518 (1953).
16. Watson, E. A., Joseph Lucas Res. Lab., *Rept. No. L. 1675* (1945).
17. Te-Nuyl, J. A., *B.P.M. Lab. Amsterdam*, private communication, (1945).
18. Harvey, J. F., and A. S. Hermandorfer, *Trans. Soc. Nav. Arch. Marine Eng.*, **51**, 61 (1943).
19. Watson, E. A., Joseph Lucas Res. Lab., *Rept. No. L. 1258* (1944).
20. Ibid., *Rept. No. L. 2671* (1947).
21. Novikov, I. I., *J. Tech. Phys. U.S.S.R.*, **18**, 345 (1948); English Trans. in Eng. Digest, **10**, 72 (1949).
22. Sohngen, F., and U. Grigull, *Forschung Gebiete Ing.*, **17**, 77 (1951).

Manuscript received October 26, 1967; revision received April 9, 1968; paper accepted April 10, 1968.